

Halogen Bonding Promotes Higher Dye-Sensitized Solar Cell Photovoltages

Sarah J. C. Simon,[†] Fraser G. L. Parlane,[†] Wesley B. Swords,[‡] Cameron W. Kellett,[†] Chuan Du,[†] Brian Lam,[†] Rebecca K. Dean,[†] Ke Hu,[‡] Gerald J. Meyer,^{*,‡} and Curtis P. Berlinguette^{*,†}

[†]Departments of Chemistry and Chemical & Biological Engineering, The University of British Columbia, 2036 Main Mall, Vancouver, BC V6T 1Z1, Canada

[‡]Department of Chemistry, The University of North Carolina at Chapel Hill, Murray Hall 2202B, Chapel Hill, North Carolina 27599-3290, United States

S Supporting Information

ABSTRACT: We report here an enhancement in photovoltage for dye-sensitized solar cells (DSSCs) where halogen-bonding interactions exist between a nucleophilic electrolyte species (I^-) and a photo-oxidized dye immobilized on a TiO_2 surface. The triarylamine-based dyes under investigation showed larger rate constants for dye regeneration (k_{reg}) by the nucleophilic electrolyte species when heavier halogen substituents were positioned on the dye. The open-circuit voltages (V_{OC}) tracked these k_{reg} values. This analysis of a homologous series of dyes that differ only in the identity of two halogen substituents provides compelling evidence that the DSSC photovoltage is sensitive to k_{reg} . This study also provides the first direct evidence that halogen-bonding interactions between the dye and the electrolyte can bolster DSSC performance.

The reduction of a photo-oxidized dye immobilized on a TiO_2 surface by a soluble reductant (e.g., I^-) is a critical step in the dye-sensitized solar cell (DSSC).^{1–3} The rate constant of this dye regeneration step (k_{reg} ; eq 1) needs to be larger than the rate constant of the back-electron transfer (BET) reaction between the photo-oxidized dye and electrons injected into the semiconductor, $TiO_2(e^-)$ (k_{BET} ; eq 2) in order to extract useful electrical work from the device. The interactions that exist between the reductant and the reactive portion of the oxidized dyes are expected to affect the kinetics of the dye regeneration step.⁴ For many years, the observation of nearly quantitative incident photon-to-current efficiencies led researchers to conclude that this regeneration step was not relevant to the efficiency of operational DSSCs. We and others have shown that the voltage under open-circuit conditions (V_{OC}) depends strongly on the regeneration efficiency (η_{reg} ; eq 3) and that nonquantitative regeneration near open circuit may diminish the DSSC photovoltage and power conversion efficiency (PCE).^{5,6}

dye regeneration:



back-electron transfer:



regeneration efficiency:

$$\eta_{reg} = k_{reg}[I^-]/(k_{reg}[I^-] + k_{BET}n_{TiO_2}^x) \quad (3)$$

where n_{TiO_2} is the concentration of minority carriers and x is the reaction order in $TiO_2(e^-)$ for BET.⁶

Dye–iodide interactions ostensibly play an important role in dye regeneration. However, resolving dye–electrolyte interactions in the dynamic environment of the DSSC is not trivial.^{7,8} We have previously demonstrated that modification of the donor unit, the reactive portion of the dye following light-induced charge injection into the semiconductor, influences the intermolecular interactions between the oxidized dye and iodide and yields photovoltages that increase with k_{reg} .^{5,9} The two organic donor–acceptor molecules used in our previous study differed only in the identity of the two chalcogen atoms (O or S) fixed to the triphenylamine (TPA) donor unit, thereby demonstrating that very slight differences in intermolecular forces can have a significant impact on the measured k_{reg} and V_{OC} values.⁵ This striking observation prompted us to consider whether halogen bonding could also benefit dye regeneration in the DSSC.

A halogen bond occurs when a halogen atom attached to an electron-deficient atom shows a high propensity to interact with a nucleophile due to the formation of an electropositive “ σ -hole” on the pole of the halogen atom.^{10,11} This σ -hole increases with the polarizability and principal quantum number n of the halogen valence electron shell and with the electron-withdrawing strength of the covalently bonded moiety. While fluorine is not likely to form a σ -hole, the free energy change that accompanies halogen bonding can be >10 kcal mol⁻¹ for heavier halogen substituents.¹¹

In context of the DSSC, redox-active iodide in the electrolyte serves as the nucleophile, and a heavy halogen atom on the dye bears the σ -hole. Previous use of halogen atoms in DSSC sensitizers has largely been confined to fluorination near the anchoring groups that serves to suppress the rate of charge recombination between $TiO_2(e^-)$ and the oxidized form of the electrolyte (k_{CR} ; eq 4).^{12–15} Halogen bonding is not expected to affect k_{reg} in these cases because the fluorine atoms would not contain a substantial σ -hole and are not positioned on the

Received: June 17, 2016

Published: August 12, 2016

portion of the dye that likely reacts with the electrolyte.^{16,17} Neuburger, Constable, Housecroft, and co-workers designed a series of dyes with the appropriate placement of heavy halogen atoms to facilitate halogen bonding and reported measurable

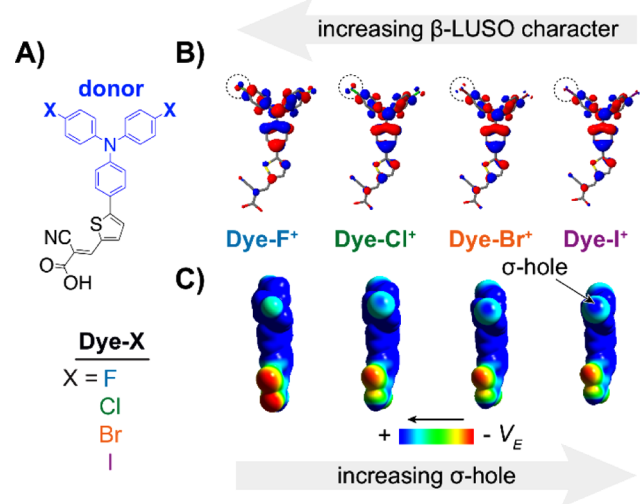


Figure 1. (A) Molecular structures of the **Dye-X** series. The donor unit is the portion of the molecule most likely to react with the electrolyte and is indicated in blue. (B, C) DFT models of the singly oxidized forms of **Dye-X** showing (B) the β -LUSO and (C) the existence of σ -holes on the poles of the terminal halogen substituents for the series, with the exception of **Dye-F**. The electrostatic potentials (V_E) are plotted from -0.0140 hartree (red) to $+0.0871$ hartree (blue) over the total electron densities at an absolute isovalue of 0.001 .

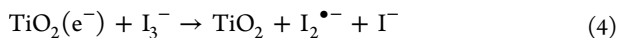
Table 1. Photovoltaic Parameters for Devices Containing an Iodide-Based Electrolyte^a

dye	PCE (%)	V_{OC} (mV)	J_{SC} (mA cm ⁻²)	FF
Dye-F	5.7 ± 0.7	720 ± 9	12.1 ± 0.2	0.70 ± 0.06
Dye-Cl	5.2 ± 0.1	709 ± 4	12.1 ± 0.2	0.63 ± 0.01
Dye-Br	5.5 ± 0.2	717 ± 2	11.9 ± 0.4	0.66 ± 0.02
Dye-I	6.5 ± 0.2	740 ± 7	12.0 ± 0.7	0.75 ± 0.02

^aThe iodide electrolyte solution was composed of 0.6 M 1,3-dimethylimidazolium iodide (DMII), 40 mM I₂, 0.5 M *tert*-butylpyridine, 0.03 M NaI, and 0.1 M GuNCS in a mixed-solvent system of acetonitrile and valeronitrile (85:15 v/v). The averages and standard deviations reported include data for no fewer than four devices; statistical outliers were excluded.

differences in DSSC device characteristics, which suggests that this intermolecular interaction may indeed play a beneficial role.¹⁸

charge recombination with electrolyte:



In a previous study, a series of four dyes differing only in the identity of the two halogen substituents covalently attached to the TPA donor unit (**Dye-X**, where X = F, Cl, Br, I; **Figure 1A**) immobilized on TiO₂ displayed enhanced k_{reg} due to halogen bonding when heavier halogens were used.¹⁹ Here we extend this result into fully functional DSSC devices, where we demonstrate that this improvement in k_{reg} has a measurable effect on cell performance (**Table 1**). The V_{OC} values were found to increase by ~ 40 mV for the **Dye-X** series bearing the more polarizable substituents, and since the short-circuit

Table 2. Optical, Thermodynamic, and Kinetic Data Relevant to Dye Regeneration by Iodide

dye	λ_{max} (nm) ^a	E° (V) ^b	k_{reg} (10 ⁸ M ⁻¹ s ⁻¹) ^c	ΔG° (V) ^{d,e}	ΔG° (V) ^{d,f}
Dye-F	432	1.22	4.7	0.01	-0.43
Dye-Cl	420	1.27	8.8	-0.04	-0.48
Dye-Br	429	1.28	10.9	-0.05	-0.49
Dye-I	432	1.27	13.5	-0.04	-0.48

^aMaximum of the lowest-energy absorption band, recorded in MeCN.¹⁸ ^bMeasured in 0.3 M NaClO₄/MeCN electrolyte at 100 mV s⁻¹ and externally referenced to Fc/Fc⁺ prior to adjustment by +0.64 V vs NHE.¹⁸ ^cRecorded in MeCN solutions at various I⁻ concentrations.¹⁸ ^dOne-electron iodide oxidation may occur through two different mechanisms, one that is first-order in I⁻ and generates I[•], and one that is pseudo-first-order in I⁻ and yields I₂^{•-}. The latter mechanism is generally thought to be operative in DSSCs and is shown in **Figure 2**. ^eCalculated free energy change for outer-sphere reactions based on $E^\circ(\text{Dye-X}^+/\text{Dye-X})$ and 1.23 V for $E^\circ(\text{I}^\bullet/\text{I}^-)$.⁵ ^fCalculated free energy change for outer-sphere reactions based on $E^\circ(\text{Dye-X}^+/\text{Dye-X})$ and 0.79 V for $E^\circ(\text{I}_2^{\bullet-}/2\text{I}^-)$.²¹

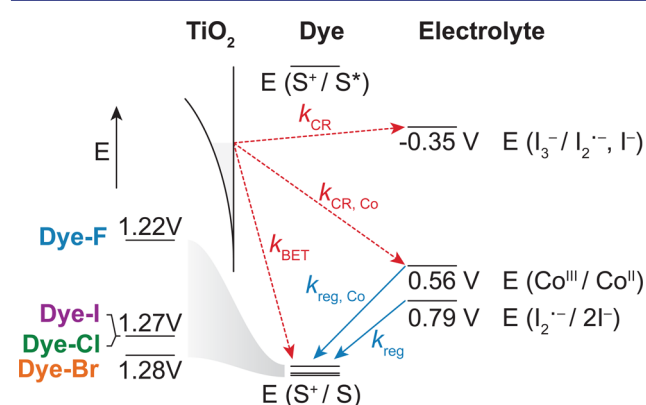


Figure 2. Energy level diagram describing key interfacial charge recombination (k_{CR}), back-electron transfer (k_{BET}), and dye regeneration (k_{reg}) processes and showing the relevant energy levels for **Dye-X** and iodide and cobalt containing electrolytes. S indicates **Dye-X**. All potentials are vs NHE.

current densities (J_{SC}) were held at parity, the PCE values also increased for the series.

The redox and optical properties of the **Dye-X** series have been reported previously and are summarized in **Table 2**.¹⁹ The quasi-reversible TPA^{•+}/TPA⁰ redox couples were within the TiO₂ electrochemical window with extremes of 1.22 V (**Dye-F**) and 1.28 V (**Dye-Br**) (all potentials herein are referenced vs NHE). These data indicate that the electronic structures of the dyes are not significantly perturbed by the identity of halogen atoms, thereby enabling the interfacial reactivity to be quantified without appreciable differences in driving force (ΔG° ; **Table 2**). The absorbance profiles for the series revealed a band with a maximum at ~ 425 nm corresponding to the $\pi \rightarrow \pi^*$ transition from the TPA to the cyanoacrylic acid moiety.⁵ The λ_{max} values of the singly oxidized dyes shift to the red with increasing halogen size and fall in the range ~ 605 – 625 nm. The excited-state reduction potentials, $E(S^+/S^*)$, were calculated to be approximately -1.2 V for the series on the basis of the E_{0-0} value obtained from the intersection of the ground-state absorbance and emission spectra (**Figures S3 and S4**) and are therefore accommodating to light-induced electron injection into the semiconductor.^{3,20}

Table 3. Photovoltaic and Kinetic Data for Devices with Cobalt-Based Electrolytes^a

dye	PCE (%) ^b	V _{OC} (mV)	J _{SC} (mA cm ⁻²)	FF	k _{reg,Co} (10 ⁷ M ⁻¹ s ⁻¹) ^c	ΔG° (V) ^d
Dye-F	5.5 ± 0.2	738 ± 7	11.6 ± 0.4	0.64 ± 0.08	2.8	-0.66
Dye-Cl	5.3 ± 0.1	735 ± 5	11.7 ± 0.3	0.62 ± 0.01	4.4	-0.71
Dye-Br	5.5 ± 0.1	737 ± 4	11.9 ± 0.3	0.63 ± 0.01	7.2	-0.72
Dye-I	5.4 ± 0.2	740 ± 10	11.2 ± 0.1	0.65 ± 0.02	5.4	-0.71

^aThe electrolyte was composed of 0.02 M [Co(bpy)₃](PF₆)₃, 0.2 M [Co(bpy)₃](PF₆)₂, 0.1 M LiClO₄, and 0.2 M *tert*-butylpyridine dissolved in MeCN. ^bThe averages and standard deviations reported include data for no fewer than four devices; statistical outliers were excluded. ^cData were recorded in 0.3 M NaClO₄/MeCN solutions at various [Co(bpy)₃]²⁺ concentrations. ^dCalculated free energy change for outer-sphere reactions based on E°(Co^{III}/Co^{II}) = 0.56 V.

The rate constant of BET to the oxidized dyes ($k_{\text{BET}} = 130 \text{ s}^{-1}$; eq 2), as previously quantified by nanosecond transient absorption measurements, was insensitive to the presence of the halogen atoms.¹⁹ Dye-F showed an anomalously high V_{OC} that is typically ascribed to a suppression of k_{CR} resulting from the exclusion of electrolyte from the semiconductor surface,^{11–14} but this assertion is not supported by our experimental data. The rate constants for charge recombination from injected electrons to the electrolyte (k_{CR} , eq 4) were the same within experimental error for all of the dyes (Table S1). This collection of data nonetheless implicates faster dye regeneration as the origin of the higher photovoltages for the heavier substituents.

Computational modeling, which is widely used to describe halogen bonding,^{22–25} was performed on the Dye-X⁺ compounds and confirmed that a σ -hole is indeed present opposite the covalently bound carbon on the heavier halogen atoms Cl, Br, and I (Figure 1C) and that the size of the σ -hole increases proportionally with the halogen polarizability.¹⁹ Dye-F⁺ showed a negligible σ -hole in the oxidized form, as expected. The lowest unoccupied β spin orbital (β -LUSO) of the Dye-X⁺ compounds shows the most orbital character on the halogen substituents in Dye-F⁺ and decreasing character with heavier halogens (Figure 1B), indicating that the positive charge upon photo-oxidation is more delocalized onto smaller halogen atoms.⁵ This finding is expected given that the carbon π -system is better matched to overlap with the fluorine valence 2p electrons than those of the larger halogens.

Quantum-mechanical models were previously utilized to observe the proposed Dye-X⁺⋯I⁻ halogen-bonding interactions in the ground state,¹⁹ which we have extended here to include Dye-X⁺⋯I⁻ interactions, which better represent dye regeneration. The energies of these interactions (ΔE_{int}) were obtained by comparing the energies of these interacting systems to those of the noninteracting pairs, as described in the Supporting Information. The value of ΔE_{int} was found to be 3.0 kcal mol⁻¹ lower for Dye-I⁺ than for Dye-F⁺, with a concomitant 0.65 Å contraction in internuclear distances (Table S2). The interaction distances ($d_{\text{X}\cdots\text{I}}$) were calculated to be shorter than predicted from the van der Waals radii for Dye-Cl⁺, Dye-Br⁺, and Dye-I⁺, while the values for Dye-F⁺ were beyond the predicted van der Waals distances. These data indicate that halogen bonding can exist between iodide and Dye-Cl⁺, Dye-Br⁺, and Dye-I⁺, with increasing halogen-bonding character for the larger polarizable halogen atoms bearing the larger σ -holes for the series. Natural bond orbital (NBO) analysis describes the principal Dye-X⁺⋯I⁻ interaction as a Lewis acid–base adduct between a lone pair on iodide and the empty C–X σ^* orbital. A significant increase in the stabilization energy of this interaction (E^2) was predicted for heavier halogen-bonding

substituents (Table S3), lending credence to halogen-bonding interactions.

We modeled scenarios where iodide approaches the oxidized dye from directions other than the C–X vector, including being juxtaposed to the phenyl rings (Figure S9 and Tables S4 and S5) as well as the nitrogen atom of the TPA unit (Figure S10 and Table S6). Intermolecular interactions at both positions were calculated to be stronger than halogen bonding as a result of the Coulombic attraction between I⁻ and the positively charged TPA moiety, but these interactions were not sensitive to the halogen substituents (Figure S11). This outcome points to the extent of halogen bonding being responsible for the differences in V_{OC} for the series.

We repeated the preceding series of experiments using a cobalt-based electrolyte. Halogen bonding is not expected to be operative during dye regeneration by the cationic [Co(bpy)₃]²⁺ species, which therefore serves as a valuable control for contrasting the purported intermolecular interaction with iodide. The V_{OC} values were generally higher for devices containing the cobalt electrolyte because of the more positively shifted [Co(bpy)₃]^{3+/2+} reduction potential relative to I₃⁻/3I⁻ (Figure 2). More importantly, the measured V_{OC} values were within experimental error for the same Dye-X series with the cobalt electrolyte (Table 3). Regeneration kinetic data also did not indicate reduction of Dye-X⁺ by [Co(bpy)₃]²⁺ to be more favorable for Dye-I. Instead, the data more closely tracked the free energy change for the reaction between Dye-X⁺ and [Co(bpy)₃]²⁺ (Table 3 and Figure S5) and not the size of the σ -hole for the oxidized dyes (Figure 1C). The rate of charge recombination between the semiconductor and [Co(bpy)₃]³⁺ ($k_{\text{CR,Co}}$) was equivalent for the series and therefore was not responsible for the differences in measured photovoltages. These experiments do not reveal any kinetic advantage in changing the halogen substituent on the dye when the cobalt electrolyte is used, which is in sharp contrast to measurements with the iodide electrolyte.

In summary, a new approach for optimizing the critical regeneration step in DSSCs has been discovered that exploits the highly polarizable nature of iodide and the Lewis acidity of organoiodide σ -holes carefully positioned about the sensitizing dyes. Hence, this Communication provides the first direct evidence that halogen bonding can be utilized to optimize the open-circuit voltage and, by extension, the maximum power conversion efficiency of regenerative solar cells.

■ ASSOCIATED CONTENT

📄 Supporting Information

The Supporting Information is available free of charge on the ACS Publications website at DOI: 10.1021/jacs.6b06288.

Experimental details and additional data (PDF)

■ AUTHOR INFORMATION

Corresponding Authors

*gjmeyer@email.unc.edu

*cberling@chem.ubc.ca

Notes

The authors declare no competing financial interest.

■ ACKNOWLEDGMENTS

UNC authors acknowledge support from the Division of Chemical Sciences, Office of Basic Energy Sciences, Office of Energy Research, U.S. Department of Energy (Grant DE-SC0013461) and the National Science Foundation Graduate Research Fellowship Program (Grant DGE-1144081 to W.B.S). UBC authors are grateful for support from the Canadian Natural Sciences and Engineering Research Council, the Canadian Foundation for Innovation, CIFAR, and Canada Research Chairs.

■ REFERENCES

- (1) O'Regan, B.; Grätzel, M. *Nature* **1991**, 353 (6346), 737.
- (2) Hagfeldt, A.; Boschloo, G.; Sun, L.; Kloo, L.; Pettersson, H. *Chem. Rev.* **2010**, 110, 6595.
- (3) Ardo, S.; Meyer, G. J. *Chem. Soc. Rev.* **2009**, 38 (1), 115.
- (4) O'Regan, B. C.; López-Duarte, I.; Martínez-Díaz, M. V.; Forneli, A.; Albero, J.; Morandeira, A.; Palomares, E.; Torres, T.; Durrant, J. R. *J. Am. Chem. Soc.* **2008**, 130 (10), 2906.
- (5) Robson, K. C. D.; Hu, K.; Meyer, G. J.; Berlinguette, C. P. *J. Am. Chem. Soc.* **2013**, 135 (5), 1961.
- (6) Li, F.; Jennings, J. R.; Wang, Q. *ACS Nano* **2013**, 7 (9), 8233.
- (7) Clifford, J. N.; Palomares, E.; Nazeeruddin, Md. K.; Grätzel, M.; Durrant, J. R. *J. Phys. Chem. C* **2007**, 111 (17), 6561.
- (8) Tuikka, M.; Hirva, P.; Rissanen, K.; Korppi-Tommola, J.; Haukka, M. *Chem. Commun.* **2011**, 47 (15), 4499.
- (9) Hu, K.; Severin, H. A.; Koivisto, B. D.; Robson, K. C. D.; Schott, E.; Arratia-Perez, R.; Meyer, G. J.; Berlinguette, C. P. *J. Phys. Chem. C* **2014**, 118 (30), 17079.
- (10) Bui, T. T. T.; Dahaoui, S.; Lecomte, C.; Desiraju, G. R.; Espinosa, E. *Angew. Chem., Int. Ed.* **2009**, 48 (21), 3838.
- (11) Metrangolo, P.; Meyer, F.; Pilati, T.; Resnati, G.; Terraneo, G. *Angew. Chem., Int. Ed.* **2008**, 47 (33), 6114.
- (12) Chen, D.-Y.; Hsu, Y.-Y.; Hsu, H.-C.; Chen, B.-S.; Lee, Y.-T.; Fu, H.; Chung, M.-W.; Liu, S.-H.; Chen, H.-C.; Chi, Y.; Chou, P.-T. *Chem. Commun.* **2010**, 46 (29), 5256.
- (13) Lin, Y.-D.; Chow, T. J. *J. Photochem. Photobiol., A* **2012**, 230 (1), 47.
- (14) Zhou, D.; Cai, N.; Long, H.; Zhang, M.; Wang, Y.; Wang, P. *J. Phys. Chem. C* **2011**, 115 (7), 3163.
- (15) Bonnier, C.; Machin, D. D.; Abdi, O. K.; Robson, K. C. D.; Koivisto, B. D. *Org. Biomol. Chem.* **2013**, 11 (40), 7011.
- (16) Bomben, P. G.; Robson, K. C. D.; Koivisto, B. D.; Berlinguette, C. P. *Coord. Chem. Rev.* **2012**, 256 (15–16), 1438.
- (17) Bomben, P. G.; Robson, K. C. D.; Sedach, P. A.; Berlinguette, C. P. *Inorg. Chem.* **2009**, 48 (20), 9631.
- (18) Malzner, F. J.; Brauchli, S. Y.; Constable, E. C.; Housecroft, C. E.; Neuburger, M. *RSC Adv.* **2014**, 4 (89), 48712.
- (19) Swords, W. B.; Simon, S. J. C.; Parlani, F. G. L.; Dean, R. K.; Kellett, C. W.; Hu, K.; Meyer, G. J.; Berlinguette, C. P. *Angew. Chem., Int. Ed.* **2016**, 55 (20), 5956.
- (20) Grätzel, M. *Inorg. Chem.* **2005**, 44 (20), 6841.
- (21) Boschloo, G.; Gibson, E. A.; Hagfeldt, A. *J. Phys. Chem. Lett.* **2011**, 2 (24), 3016.
- (22) Kolář, M. H.; Hobza, P. *Chem. Rev.* **2016**, 116 (9), 5155.
- (23) Rosokha, S. V.; Stern, C. L.; Ritzert, J. T. *Chem. - Eur. J.* **2013**, 19 (27), 8774.
- (24) Politzer, P.; Murray, J. S.; Clark, T. *Phys. Chem. Chem. Phys.* **2010**, 12 (28), 7748.

(25) Clark, T.; Hennemann, M.; Murray, J. S.; Politzer, P. *J. Mol. Model.* **2007**, 13 (2), 291.